C_{60} on impurity phases of the 2–fold surface of the Al–Pd–Mn quasicrystal

Journal of Physics: Conference Series **1458** (2020) 012015 doi:10.1088/1742-6596/1458/1/012015

C_{60} on impurity phases of the 2–fold surface of the Al–Pd–Mn quasicrystal

Sam Coates[1,2], Hem Raj Sharma[2] and Ronan McGrath[2]

[1]Department of Materials Science and Technology, Tokyo University of Science, 6 Chome–3–1 Niijuku, Katsushika City, Tokyo, 125-8585, Japan
[2]Surface Science Research Centre, Department of Physics, University of Liverpool, Liverpool, L69 3BX, UK

E-mail: hemraj@liv.ac.uk

Abstract. Using STM, we show several off-stoichiometric impurity phases detected at the 2–fold Al–Pd–Mn quasicrystal surface. By comparing the observed surface structure to planes from similar bulk phases in the Al–Pd system, we identify these phases as β–Al–Pd and Pd_5Mn_3. C_{60} is adsorbed at these domains, forming simple hexagonal close packed (hcp) structures. We identify potential adsorption schemes, and compare the adsorption behaviour to C_{60} on the quasicrystalline phase.

1. Introduction

Recently, we showed that the 2–fold surface of an icosahedral (i–)$Al_{70.2}Pd_{21.5}Mn_{8.3}$ quasicrystal can be used as a template for pseudomorphic growth of C_{60}, resulting in a Fibonacci square grid structure [1]. During this investigation several periodic impurity surface domains were detected, each observed after using the same preparation conditions to produce the quasicrystalline surface. Previously, an orthorhombic phase was observed upon the same sample surface, although a detailed discussion of its origin was not undertaken [2]. This orthorhombic phase showed a row structure, and was thought to be an off–QC–stoichiometric H phase ($Al_{75}Pd_6Mn_{19}$), which had also been seen on the 5–fold surface [3, 4]. However, as is the case in this work, the size of these domains on the sample was on the order of 100 nm or less, so that elemental analysis of their composition (by using X-ray photoelectron spectroscopy, for example) is not possible.

Here, we identify possible phases of these periodic areas by comparing the surface structure to crystallographic data of stoichiometrically similar materials. These possible phases are Mn deficient. Likewise, we highlight the difference in adsorption behaviour of C_{60} between the quasicrystalline and periodic phases. In the Fibonacci square grid work, preferential adsorption behaviour was attributed to a sparse Mn network. The images shown here display no such preference.

2. Experimental Methods

The 2–fold i–Al–Pd–Mn surface was prepared by polishing with diamond paste of successively finer grades (6–0.25 μm) before washing with methanol in an ultrasonic bath. After insertion into a UHV chamber, the surface was further cleaned and prepared by cycles of sputter–annealing (30 min Ar^+ sputter, 2 hour anneal at 900 K). The surface was characterised by low energy

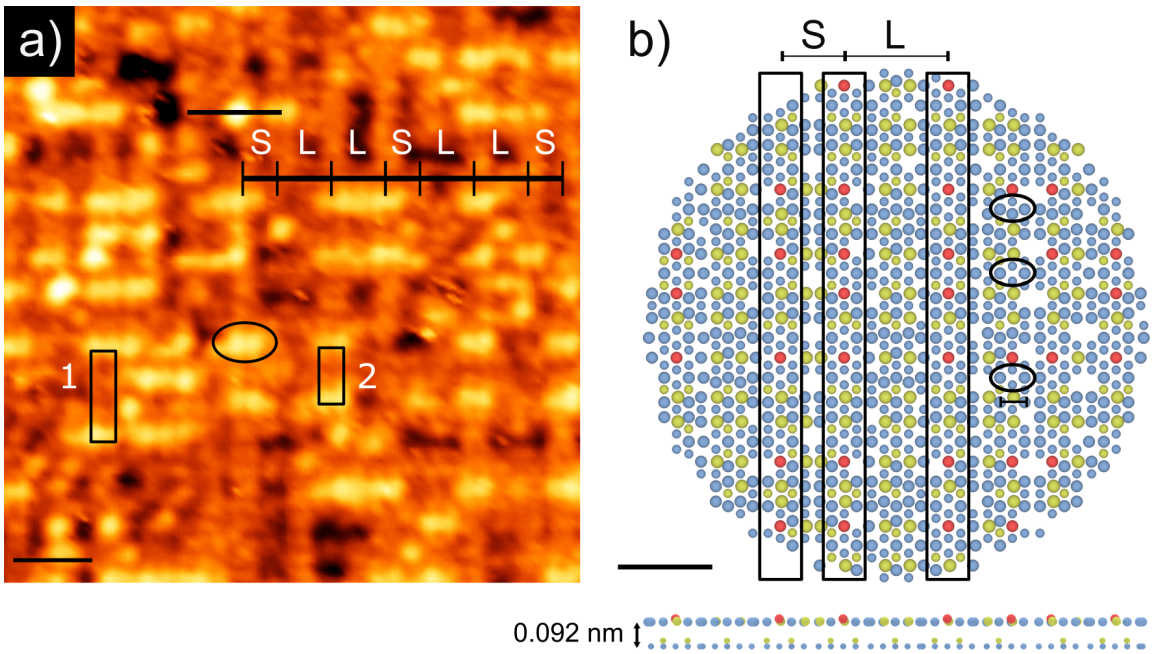

Figure 1. (a) STM image (V_b = 1 V, I_t = 292 nA) of the clean 2–fold surface of the *i*–Al–Pd–Mn quasicrystal. Rows are separated by a Fibonacci sequence (some of rows are marked by lines). Bright protrusions (dimers) sit on top of these rows, separated by values related to the row separation by τ. Scale bar is 3nm. The highlighted motifs will be discussed in the text. (b) A model schematic shows these features, with blue atoms = Al, yellow = Pd, and red = Mn. The separation between two surface planes is shown below. Scale bar is 2nm.

electron diffraction (LEED) and scanning tunnelling microscopy (STM). The bias voltage to the sample (V_b) and tunneling current (I_t) for each STM image are given in Figure captions. C_{60} was deposited by thermal evaporation with the substrate held at 600 K.

3. Results

3.1. Quasicrystalline phase

Figure 1(a) is an STM image of the clean 2–fold surface, which shows a clear row structure. A section of selected rows have been marked with a Fibonacci sequence, where $S = 1.25 \pm 0.02$ nm and $L = 2.02 \pm 0.02$ nm. L/S gives 1.62 $\pm$0.03, matching well with the golden ratio $\tau = 1.618...$, an indicator of quasiperiodic order. Sitting on top of these rows are bright protrusions – these bright spots most often appear as dimers with an example marked by an oval. The separation of the individual protrusions which make the dimers is 0.49 ± 0.02 nm. The dimers are themselves separated along the direction of the rows by two common distances 3.25$\pm$0.03 nm and 2.02$\pm$0.03 nm, marked as 1 and 2 respectively. Again, these are related by τ. Larger or smaller (τ–scaled) separations are also occasionally observed. The length–scales of the row separations and perpendicular structures is τ, as expected from the 2–fold symmetry of the system [1].

These surface features can be explained using two closely separated planes of the bulk model proposed by Boudard et al. [5], shown in Figure 1(b). Here, Al atoms are blue, Pd are yellow, and Mn are red. Marked by ovals are dimers of Al atoms from the top surface layer, which are separated by 0.484 nm, in agreement with the separation of the dimers in Figure 1(a). The model dimers sit on top of rows of the bottom surface layer, which are separated by $S = 1.26$ nm (marked in Figure 1(b)), and $L = 2.04$ nm. Again this is in agreement with STM. Finally, the height difference between these two surface planes is 0.092 nm, which matches the height of

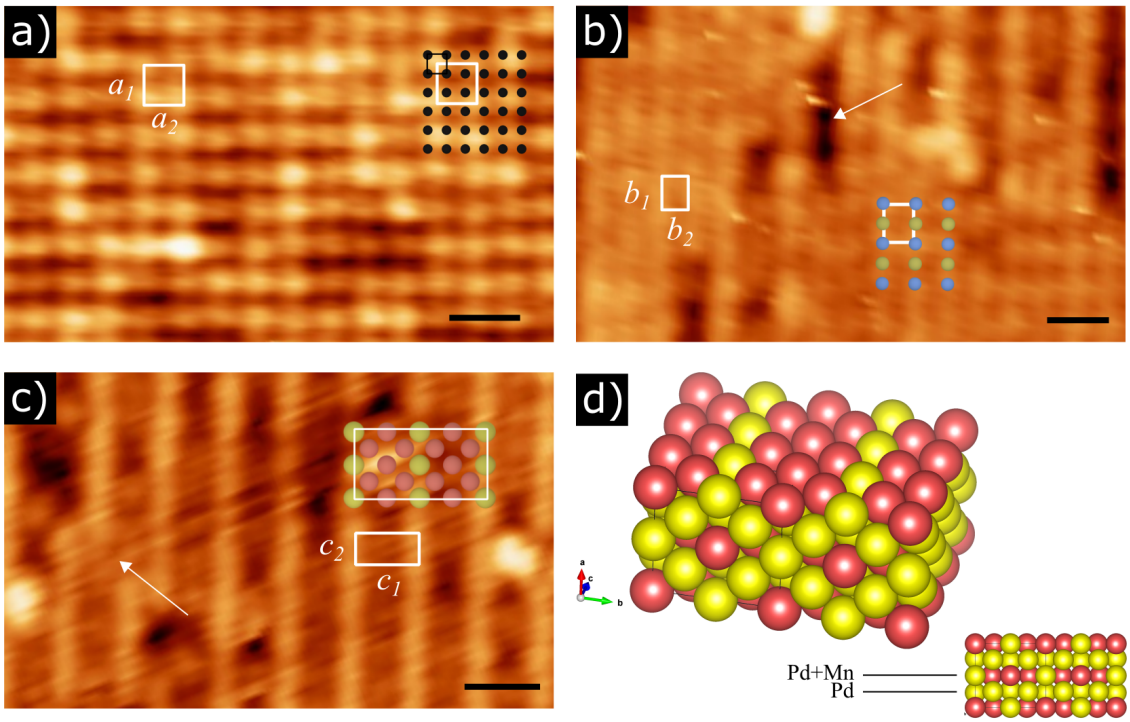

Figure 2. (a) STM image (V_b = -0.7 V, I_t = 292 nA) of the (100) surface of the β–Al–Pd phase. A square unit cell is highlighted, along with a model of the surface (black). Scale bar is 1 nm. (b) STM image (V_b = -0.7 V, I_t = 292 nA) of the (112) surface of the β–Al–Pd phase. A unit cell is highlighted, with a model schematic also overlaid. Blue is Al, yellow is Pd. An arrow indicates a defect site. Scale bar is 1 nm. (c) STM image (V_b = -0.7 V, I_t = 292 nA) of the (100) surface of the Pd_5Mn_3 phase. A unit cell and model schematic are highlighted. An arrow points to a row switch defect. Scale bar is 1 nm. (d) A model of the orthogonal Pd_5Mn_3 phase with cell parameters $a = 0.728$ nm, $b = 0.807$ nm, $c = 0.404$ nm. Inset shows the composition of planes along c.

the Al dimers above the median substrate in Figure 1(a), 0.089 ± 0.004 nm.

3.2. Periodic phases

We obtained STM images from the surface which showed structures that are not expected from the 2–fold Al–Pd–Mn quasicrystal surface. These images are shown in Figures 2(a–c). We consider these structures to result from impurity phases of quasicrystalline Al–Pd–Mn. Such impurity phases may be produced in the sample during growth [6]. Likewise, the phase diagram of ternary Al–Pd–Mn shows several ternary extensions of binary phases which are in equilibrium with the icosahedral phase, both below and above the annealing temperature used [7]. We identify the structure in Figures 2(a, b) as facets from the body–centered–cubic (space group 195) β–Al–Pd phase. Indeed, metastable films of this phase have previously been observed at the i–Al–Pd–Mn surface after sputtering of high–symmetry orientations [8, 9].

The β–Al–Pd phase has a lattice constant of 0.304 – 0.306 nm [11]. The unit cell of the square–like facet measured in Figure 2(a) has vectors $a_1 = 0.64 \pm 0.02$ nm and $a_2 = 0.62 \pm 0.02$ nm, matching well with double the β–Al–Pd lattice constant ($\pm 3\%$). Therefore, this domain is identified as the (100) surface of β–Al–Pd, where clusters or groups of atoms are represented by each protrusion, as indicated by the dark circles in Figure 2(a).

The second facet of the β–Al–Pd phase is shown in Figure 2(b). This domain has a row structure, with a marked unit cell of $b_1 = 0.56 \pm 0.08$ nm and $b_2 = 0.42 \pm 0.02$ nm. Defect (partially missing) rows appear with regularity, as marked by a white arrow. These b_1 and b_2 values and the row structure match with the (112) plane of the β–Al–Pd phase, which is comprised of rows of alternating Al/Pd atoms. An example is overlaid on Figure 2(b), where Al is blue, Pd is yellow. The unit cell of the overlaid model structure (marked in white) is given by $b_1 = 0.528$ nm and $b_2 = 0.431$ nm. If we consider that only Al or Pd are observed by STM, this model fits well with the measured unit cell values ($\pm 6\%$). Bias dependency experiments were not conducted as part of this study, however, STM contrast difference is often expected between the constituents of transition metal aluminides due to differing contributions to the density of states [10]. Likewise, it could be that Al–Pd dimers are resolved as single protrusions, which would again fit well with the measured values.

Finally, Figure 2(c) shows another row structure, with alternating bright/dark rows. Occasionally rows will 'switch' from bright to dark, as marked by a white arrow. A unit cell is indicated, where $c_1 = 0.85 \pm 0.01$ nm and $c_2 = 0.45 \pm 0.03$ nm. This domain is thought to be the (100) surface from the Pd_5Mn_3 phase. Pd_5Mn_3 is orthogonal (space group 65) with unit cell parameters of $a = 0.728$ nm, $b = 0.807$ nm, $c = 0.404$ nm, shown in Figure 2(d) [12]. The [100] direction consists of mixed planes of Pd/Mn separated by planes of pure Pd. The mixed planes create a row structure with both Mn and Pd forming rows. The atoms within these rows have partial occupancy (0.84 for Pd, 0.88 for Mn). An example of the mixed plane structure is shown in Figure 2(c), where Pd has been chosen as the constituent contributing to bright contrast (Mn is red, Pd is yellow). The Pd rows in the model have a unit cell of $c_1 = 0.81$ nm and $c_2 = 0.40$ nm, matching with the measured unit cell ($\pm 12\%$). The bright/dark row structure observed could either be bias dependent, or a desorption of the intermediate Mn rows. Likewise, the row 'switching' could be an effect of the partial occupancy of the Pd and Mn positions, whereby one Pd (Mn) atom occupies a Mn (Pd) site, possibly inducing a row switch.

3.3. C_{60} on periodic phases

C_{60} adsorption was observed on the β–Al–Pd(112) and Pd_5Mn_3(100) domains. Figure 3(a) shows the β–Al–Pd(112) phase, where C_{60} grows in a hcp structure with an overall orientation commensurate with the underlying row structure of the substrate. A large arrow indicates that the C_{60} appears to sit between the observed rows. The labelled unit cell parameters are $a = 0.96 \pm 0.07$ nm, $b = 1.01 \pm 0.04$ nm and $\gamma = 122 \pm 2^\circ$. Figure 3(b) shows a model schematic considering these values. Here, a hcp superstructure can be formed by bridge sites between four atoms – two Al, two Pd. The resultant hcp lattice is marked, with $a = 1.06$ nm, $b = 1.01$ nm and $\gamma = 121.5^\circ$, a good fit with the experimental values.

Figure 3(c) shows C_{60} on the Pd_5Mn_3(100) phase. Here, two structure types are observed. The first is a hcp domain with parameters $a = 1.00 \pm 0.07$ nm, $b = 1.03 \pm 0.05$ nm and $\gamma = 123 \pm 2^\circ$. Again, this phase appears commensurate with the row structure of the substrate. The second is a parallel C_{60} row structure which appears to separate two hcp domains. The separation of these rows is 1.25 ± 0.05 nm. Here, the row structure of the substrate appears to switch from bright to dark (and vice versa), as indicated by the two arrows. Presumably these C_{60} are adsorbing at or near defect sites highlighted by a white arrow in Figure 2(c), which shows a row 'switch'. The change in structure of the C_{60} shows that the defect sites which induce the surface row reconstruction provide a different adsorption landscape than a defect–free substrate.

An adsorption schematic is shown in Figure 3(d), which shows how both hcp and parallel structure can be formed. C_{60} forming the hcp structure sit at sites along the Pd rows, either on top of Pd atoms or within square hollow sites. The two types of sites are indicated by the hcp unit vectors (right). The parallel C_{60} row structure is adjacent on the left, with the C_{60} sitting at the same type of sites. However, in this instance the defect row structure has

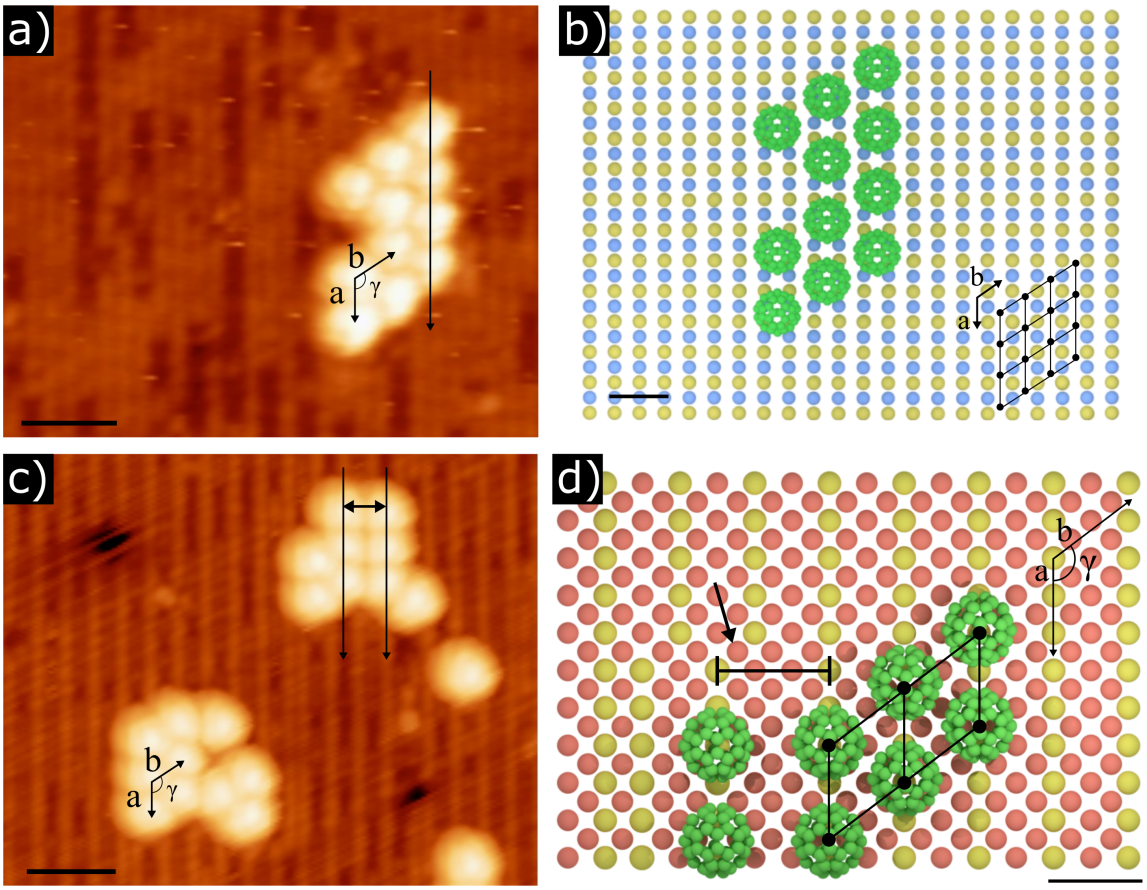

Figure 3. (a) STM image (V_b = -0.7 V, I_t = 292 nA) of C_{60} adsorbed on the β–Al–Pd (112) surface. The vectors indicate the hcp unit cell of the C_{60}. An arrow indicates that the C_{60} molecules sit in between rows of the substrate. Scale bar is 2 nm. (b) A model schematic of the adsorption scheme of (a). Scale bar is 1 nm. (c) STM image (V_b = -0.7 V, I_t = 292 nA) of C_{60} adsorbed on the Pd_5Mn_3 surface. Again unit cell vectors of a hcp phase are highlighted, whilst a C_{60} parallel row structure is indicated by two rows. The substrate appears to switch from dark to bright along the direction of these arrows. Scale bar is 2 nm. (d) A model of the adsorption scheme in (c). Marked with a large arrow is a defect row switching site. The parallel row separation is also marked. Scale bar is 1 nm.

induced the parallel separation. The hcp lattice has parameters $a = 1.01$ nm $b = 1.01$ nm and $\gamma = 126°$, fitting the experimental values. Likewise, the row separation is 1.21 nm, matching the experimental separation of the bridge site between the hcp domains. It should be noted that the size of this separation is larger than the range of interaction between two C_{60} molecules, which strongly indicates that the parallel structure is substrate–induced.

4. Conclusions

We have tentatively identified two impurity phases, β–Al–Pd and Pd_5Mn_3, observed at the 2–fold surface of an i–Al–Pd–Mn quasicrystal. In both cases, identification was made by considering stoichiometrically similar materials to the quasicrystalline phase. For both substrates, C_{60} has been observed to adsorb in a honeycomb structure with domain orientation commensurate with the row structures of the substrate. This highlights the difference between these periodic

phases and the quasicrystalline phase. Despite the (presumed) stoichiometric similarity, the QC phase exhibits a unique adsorption network for C_{60} to form a pseudomorphic structure, whilst the periodic phases do not – showing that intermolecular forces dominate in this scheme. The comparison between the two adsorption schemes reinforces the advantageous structural/chemical properties that a quasicrystalline surface provides, in this case a unique template for creating novel thin films. This example is particularly striking given the similarity in stoichiometry between the observed phases.

References

[1] Coates S, Smerdon J A, McGrath R, and Sharma H R 2018 A molecular overlayer with the Fibonacci square grid structure *Nature Communications* **9** 3435
[2] Reid D, Smerdon J A, Ledieu J, and McGrath R 2006 The clean and copper-dosed two-fold surface of the icosahedral Al–Pd–Mn quasicrystal *Surface Science* **600** 4132
[3] Yurechko M, Grushko B, and Ebert Ph 2005 Nonicosahedral equilibrium overlayers of icosahedral quasicrystals *Phys. Rev. Lett.* **95** 256105
[4] Ledieu J, Muryn C A, Thornton G, Cappello G, Chevrier J, Diehl R D, Lograsso T A, Delaney D, and McGrath R 2000 Decomposition of the five-fold surface of $Al_{70}Pd_{21}Mn_9$ at elevated temperature *Materials Science and Engineering: A* **294** 871
[5] Boudard M, Klein H, de Boissieu M, Audier M, and Vincent H 1996 Structure of quasicrystalline approximant phase in the Al–Pd–Mn system *Philosophical Magazine A* **74** 939
[6] Sharma H R, Nugent P J, Smerdon J A, Shimoda M, Ohhashi S, Fournée V, Ledieu J, and Tsai A P 2010 Impurity phases in icosahedral Ag-In-Yb quasicrystal: Influence in surface structure *Journal of Physics: Conference Series* **226** 012004
[7] Grushko B, Yurechko M, and Tamura N 1992 A contribution to the AlPdMn phase diagram *Journal of alloys and compounds* **290** 164
[8] Fournée, V, Ross A R, Lograsso T A, Anderegg J W, Dong C, Kramer M, Fisher I R, Canfield P C, and Thiel P A 2002 Surface structures of approximant phases in the Al-Pd-Mn system *Phys. Rev. B* **66** 165423
[9] Shen Z, Kramer M J, Jenks C J, Goldman A I, Lograsso T, Delaney D, Heinzig M, Raberg W, and Thiel P A 1998 Crystalline surface structures induced by ion sputtering of Al-rich icosahedral quasicrystals *Phys. Rev. B* **58** 9961
[10] Duguet T and Thiel P A 2012 Chemical contrast in STM imaging of transition metal aluminides *Progress in Surface Science* **87** 47
[11] Villars P and Calvert L D 1985 Pearsons Handbook of Crystallographic Data for Intermediate Phases *American Society of Metals*
[12] Kádár G and Krén E 1972 Crystal and magnetic structure of the Mn_3Pd_5 phase *Solid State Communications* **11.8** 933